RSC Medicinal Chemistry

ROYAL SOCIETY OF CHEMISTRY

RESEARCH ARTICLE

View Article Online
View Journal

Cite this: DOI: 10.1039/d0md00153h

Continuous flow synthesis of lipophilic cations derived from benzoic acid as new cytotoxic chemical entities in human head and neck carcinoma cell lines†

Mabel Catalán,‡[a] Vicente Castro-Castillo,‡§[b] Javier Gajardo-de la Fuente,[b] Jocelyn Aguilera,[c] Jorge Ferreira,[a] Ricardo Ramires-Fernandez,[d] Ivonne Olmedo,[e] Alfredo Molina-Berríos,[c] Charlotte Palominos,[a] Marcelo Valencia,[a] Marta Domínguez,[f] José A. Souto*[f] and José A. Jara *[c]

Received 13th May 2020,
Accepted 30th July 2020

DOI: 10.1039/d0md00153h

rsc.li/medchem

Continuous flow chemistry was used for the synthesis of a series of delocalized lipophilic triphenylphosphonium cations (DLCs) linked by means of an ester functional group to several hydroxylated benzoic acid derivatives and evaluated in terms of both reaction time and selectivity. The synthesized compounds showed cytotoxic activity and selectivity in head and neck tumor cell lines. The mechanism of action of the molecules involved a mitochondrial uncoupling effect and a decrease in both intracellular ATP production and apoptosis induction.

1. Introduction

Delocalized lipophilic triphenylphosphonium cations (DLCs) linked to gallic acid (2,3,4-trihydroxybenzoic acid) and its derivatives have been synthesized and evaluated previously by our group, resulting in their characterization as antineoplastic compounds in a breast adenocarcinoma mouse model. All this work has allowed the identification of several lead compounds, with promising results both *in vivo* and *in vitro*.[1] It has been demonstrated that these gallic acid (GA) alkyl esters block the electron transport chain by inhibiting OXPHOS (oxidative phosphorylation).[2] Moreover, DLC–GA derivatives induce a decoupling effect, decreasing the NADH/NAD+ ratio, the mitochondrial transmembrane potential ($\Delta\Psi_m$) and ATP concentrations, consequently inducing apoptosis and antitumor effects.[1] On the other hand, DLC-benzoic acid derivatives with two hydroxyl groups, such as protocatechuic acid (3,4-dihydroxybenzoic acid) and gentisic acid (2,5-dihydroxybenzoic acid), have shown chemopreventive, cytotoxic and antiangiogenic activities in human tumor cells.[3–6] Furthermore, DLC-2,3-dihydroxybenzoic acid has shown antioxidant and antifungal activities.[7,8] Despite the promising biological results obtained, the low overall yields associated with the synthesis of these derivatives together with the long reaction times needed for their preparation are far from an optimal drug delivery process and have prevented intensive biological characterization of lead compounds (Fig. 1).

Therefore, the development of robust, efficient and reproducible synthetic protocols for the preparation of active molecules at a very early stage in the compound development pipeline warrants large quantities of material needed for the different stages of biological evaluation while increasing the speed of the eventual process of scaling up lead compounds.[9] Continuous flow processing stands out among the enabling technologies available (*e.g.* microwave assisted synthesis, high throughput catalyst screening platforms) for the synthesis of active pharmaceutical ingredients (APIs).[9–12] Advantages of this technique, compared to traditional batch procedures, include the observed enhancement of mass and heat transfer or the use of high-temperature and high-pressure reaction conditions, among others, which results in more efficient mixing of reagents and precise control of

[a] *Clinical and Molecular Pharmacology Program, Institute of Biomedical Sciences (ICBM), Faculty of Medicine, Universidad de Chile, Santiago, 8380453, Chile*
[b] *Department of Organic and Physical Chemistry, Faculty of Chemical and Pharmaceutical Sciences, Universidad de Chile, Santos Dumont 964, Santiago 8380494, Chile*
[c] *Institute for Research in Dental Sciences (ICOD), Faculty of Dentistry, Universidad de Chile, Santiago, 8380492, Chile. E-mail: jsandovalj@u.uchile.cl; Tel: +56 2 29781730*
[d] *Dentistry School, Universidad Mayor, Santiago 8340585, Chile*
[e] *Physiopathology Program, Institute of Biomedical Sciences (ICBM), Faculty of Medicine, Universidad de Chile, Santiago 8380453, Chile*
[f] *Departamento de Química Orgánica, Facultad de Química, CINBIO and IIS Galicia Sur, Universidade de Vigo, E-36310, Vigo, Spain. E-mail: souto@uvigo.es*

† Electronic supplementary information (ESI) available. See DOI: 10.1039/d0md00153h

‡ These authors contributed equally in this manuscript.

§ *In memoriam* of Dr. Vicente Castro-Castillo (1981–2019).

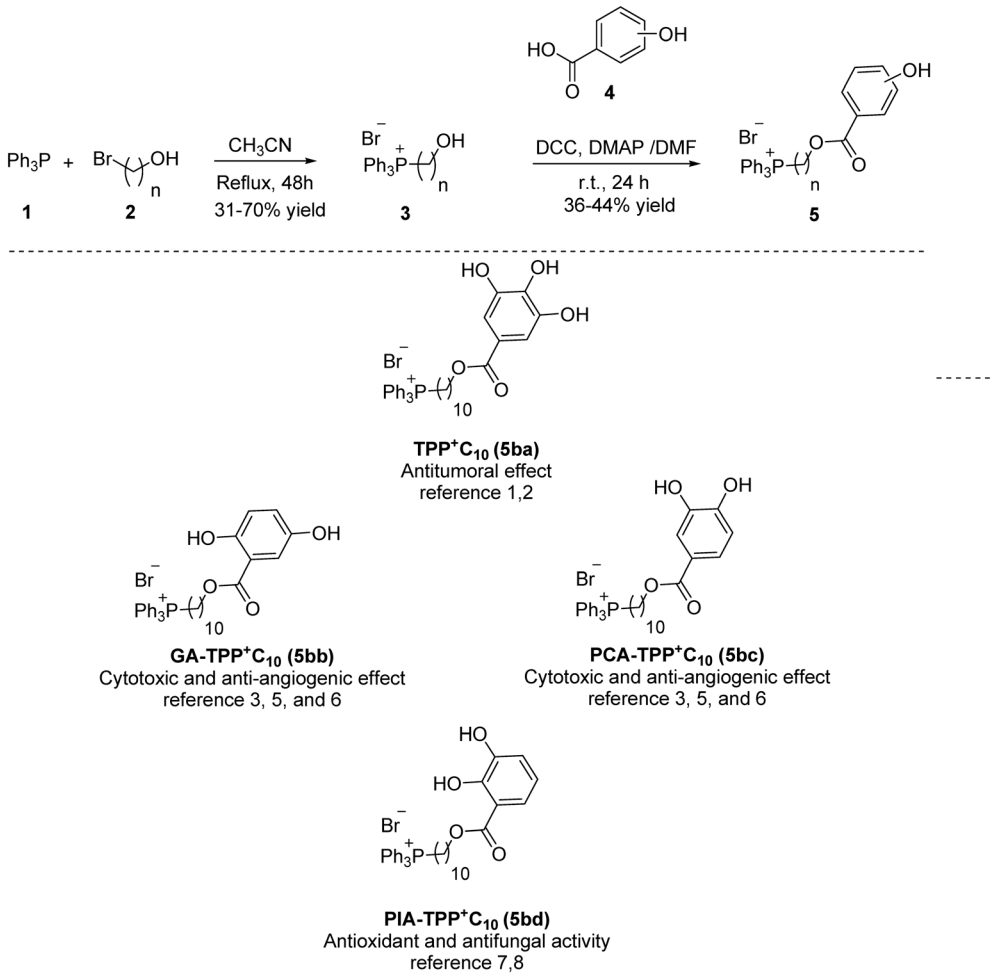

Fig. 1 A selection of DLCs previously synthesized and biologically characterized.

reaction parameters.[13–18] This results in high performance of the developed reaction in terms of reaction selectivity, product yield, low waste production and reduced cost.[11,13,19,20]

Head and neck squamous cell carcinoma (HNSCC) is one of the most common types of cancer worldwide with over 500 000 new cases reported annually.[21]

HNSCCs are a high incidence decease, and despite the progress in cancer research and therapies, the survival rate has not improved significantly in the last years, representing a continuing challenge for biomedical science, thus is a highly critical important problem for global public health, especially for dental health.

Although most of time HNSCC is considered a preventable condition, due to the possibility of early detection and treatment, the mainstream of these cancers are diagnosed in a late phase (in state III or IV). Unfortunately, in state III or IV, a combination of surgery and/or chemo/radiation therapy provides the best treatment available, these therapies produce serious adverse effects, like difficulties in talking, swallowing and performing oral hygiene, as well as increased dental caries and ulceration.[22]

Consequently, these treatments markedly lead to a significant deterioration in the patient quality of life. Furthermore, the treatment with chemotherapy has high rates of resistance. In this clinical context, the search of new molecules with antineoplastic potential it is crucial for efficacy improvement and reduce drug resistance.

Given the previously mentioned need to obtain products in high yield with short reaction times, easy purification, and chemical scalability for their biological evaluation, in the present work, we developed and optimized a telescoped, continuous-flow synthetic methodology to prepare different derivatives of poly-hydroxy-DLC esters bearing a variable number of phenolic groups.

2. Results and discussion

2.1 Chemistry

In our seminal work on the synthesis and biological characterization of DLC derivatives of polyhydroxy benzoates, we have been able to synthesize a broad number of compounds resulting in the identification of several lead molecules. That synthetic pathway contemplated as a first

step the formation of a phosphonium salt using triphenylphosphine and different bromoalcohols with various chain lengths (n = 8, 10, 11 and 12). The target compounds were isolated in moderate yields (31–70%) within 48 h. Subsequently, Steglich esterification resulted in the isolation of the desired esters, with yields ranging from 37 to 44% after 24 h of reaction. Furthermore, in both steps, chromatographic separation was necessary in order to purify the products from the secondary compounds formed during the reaction.[1]

In order to access to enough material of previously described lead compounds for further biological characterization, we initiated a study on the optimization of the previously described batch reactions under continuous flow conditions. For optimization purposes only, the commercially available and inexpensive 11-bromoundecanol **2a** was selected as the starting material (Fig. 2).

As an initial point, previously reported batch reaction conditions[1] were extrapolated to create a continuous flow regime. Hence, **2a** was dissolved in acetonitrile, and equimolar amounts of triphenylphosphine **1** were added. The resulting mixture was introduced into a 5 mL coiled reactor (0.25 mL min^{-1}, 20 min residence time), obtaining the desired product, albeit in low yield (Table 1, entry 1). Increasing the residence time to 40 min by means of reducing the flow rate and increasing the concentration of reagents slightly improved the yield of the reaction (Table 1, entries 2 and 3). Further improvement was observed when the flow rate was reduced to 0.1 mL min^{-1} and the volume of the reactor was increased (Table 1, entries 4 and 5). Surprisingly, increasing the concentration of the starting materials to near saturation resulted in higher yields for our reaction (Table 1, entries 6 and 7). Finally, an increase in the reactor temperature afforded the desired product in 92% isolated yield with a residence time of 200 min and 2.2 g h^{-1} of reaction throughput. Furthermore, the system was allowed to run for more than 5 h without any observed clogging of the reactor.

Next, we focused on the development of the esterification reaction under continuous-flow regime (Fig. 3).

For that purpose, and based on a previously described batch procedure,[1] an equimolar mixture of phosphonium salt **3a** and gallic acid **4a** in DMF merged with a solution of dicyclohexylcarbodiimide (DCC) and 4-*N*,*N*-dimethylaminopyridine (DMAP) in DMF, and the outstream liquid was introduced in a 15 mL coiled reactor at room temperature. Under these conditions, **5aa** was isolated in low yield together with secondary products that might arise by the self-reaction of activated gallic acid. Furthermore, the formation of a white precipitate caused reactor blockage after a long operation time (Table 2, entry 1). The use of CH_3CN as the solvent and a decrease in residence time did not afford satisfactory yields (Table 2, entries 2 and 3). A dramatic increase in reaction performance was obtained when a solution of **4a** in CH_3CN was reacted with another solution containing **3a**, DCC and DMAP in CH_3CN. However, despite the formation of the desired product in 70% yield, the precipitation of di-cyclohexyl urea clogged the reactor,

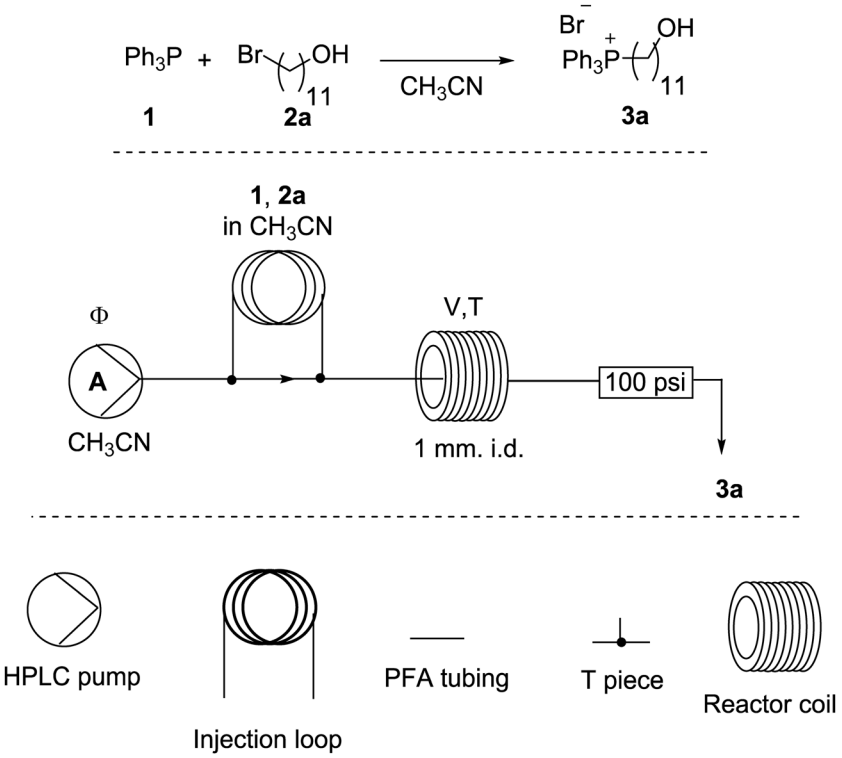

Fig. 2 Continuous flow set-up for the formation of the phosphonium salt **3a**.

Table 1 Optimization of the formation of phosphonium salt **3a**

Entry	φ (mL min^{-1})	[**1**] (M)	[**2a**] (M)	V (mL)	T (°C)	Yield[a] (%)
1	0.25	0.12	0.12	5	110	8
2	0.125	0.12	0.12	5	110	15
3	0.125	0.19	0.19	5	110	21
4	0.1	0.19	0.19	15	110	25
5	0.1	0.19	0.19	20	110	54
6	0.1	0.38	0.38	20	110	74
7	0.1	0.74	0.74	20	110	92
8	0.1	0.74	0.74	20	120	96 (92)

[a] NMR yields. Isolated yield between brackets.

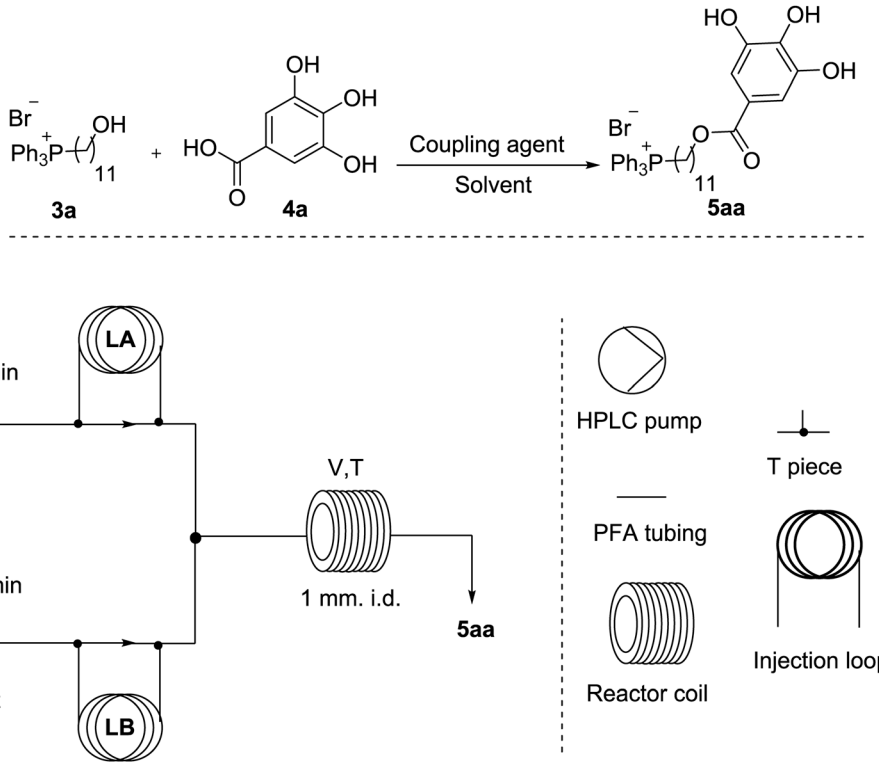

Fig. 3 Continuous flow formation of ester **5aa**.

Table 2 Optimization of the esterification reaction

Entry	Solvent	LA (x, M)	LB (x, M)	V (mL)	T (°C)	Yield[a] (%)
1	DMF	**3a**, **4a**; 0.1, 0.1	**DCC**, **DMAP**; 0.1, 0.001	15	25	11[b]
2	CH_3CN	**3a**, **4a**; 0.1, 0.1	**DCC**, **DMAP**; 0.1, 0.001	15	25	13[b]
3	CH_3CN	**3a**, **4a**; 0.1, 0.1	**DCC**, **DMAP**; 0.1, 0.001	5	25	17[b]
4	CH_3CN	**4a**; 0.1	**3a**, **DCC**, **DMAP**; 0.1, 0.1, 0.001	5	25	70[b,c]
5	CH_3CN	**4a**; 0.1	**3a**, **DCC**, **DMAP**; 0.1, 0.1, 0.001	5	50	74[b,c]
6	CH_3CN	**4a**; 0.1	**3a**, **T3P**, **TEA**; 0.1, 0.1, 0.2	5	25	82
7	CH_3CN	**4a**; 0.1	**3a**, **T3P**, **TEA**; 0.1, 0.1, 0.2	10	25	89 (85)
8	CH_3CN	**4a**; 0.1	**3a**, **T3P**, **TEA**; 0.1, 0.1, 0.2	10	50	76

[a] NMR yields. Isolated yield between brackets. [b] Reactor blockage. [c] Ultrasonic irradiation.

preventing the reaction from being carried out in this way (Table 2, entry 4). Any attempts to overcome these problems, applying different solutions previously reported in the literature to avoid clogging issues derived from particle aggregation,[23–26] were unsuccessful (Table 2, entries 4 and 5). Therefore, the coupling agent was changed to

propanephosphonic acid anhydride (T3P®), and triethylamine (TEA) was used as the base.[27] Under these conditions, we were able to isolate **5aa** in 82% yield, without any blockage of the reactor noticed (Table 2, entry 6). Increasing the residence time by doubling the reactor volume had a beneficial effect on the yield of the reaction, while increasing the temperature did not afford better results (Table 2, entries 7 and 8).

To our delight, the reaction conditions independently optimized for each step were straightforwardly telescoped for the continuous production of **5aa** without isolation of the intermediate phosphonium salt **3a**. Hence, a solution containing equimolar amounts of **1** and **2a** in acetonitrile was injected at a flow rate of 0.1 mL min^{-1} into a 20 mL reactor at 120 °C. The reactor outstream liquid merged into a 0.5 mL coiled reactor with a solution of T3P (1 equiv.) and TEA (2 equiv.) in acetonitrile (0.1 mL min^{-1}) prior to reacting with a third solution of gallic acid (1 equiv.) in acetonitrile (0.2 mL min^{-1}). The resulting mixture was introduced into a 10 mL reactor at room temperature and finally collected to afford desired product **5aa** in 74% isolated yield. Under the described reactor setup, the reactor ran for up to 5 h without obstruction (Fig. 4).

With the optimized conditions in hand for the continuous flow formation of DLC esters and considering the higher activity that DLC esters derived from 10-bromodecanol **2b** exhibit compared to derivatives of **2a**,[1] a short but representative set of already described lead DLC benzoylesters was prepared. Thus, the reaction of **2b** with different benzoic acid derivatives (**4a–e**) under the above described conditions afforded the targeted molecules, demonstrating the robustness of our methodology while affording enough material of most of the active compounds previously reported[1,3,28] for further biological characterization to be carried out (Fig. 5).

2.2 Biology

2.2.1. Cytotoxic effect of benzoic acid-derived lipophilic cations in HNSCC cell lines. The cytotoxicity results for all cell lines were plotted on a semilogarithmic graph (Fig. S1†), which allowed us to determine the concentration needed to obtain 50% cell viability (IC_{50}) for each compound assayed at 24, 48 and 72 h in human HNSCC lines and in a normal human oral keratinocyte cell line (Table 3).

The results shown in Table 3 suggest that all assayed compounds had similar IC_{50} values, approximately 2–5 μM in Cal 27 cells, 2–4.5 μM in SCC-15 cells, and 2–12 μM in HEp-2 cells. Additionally, the hydroxylated benzoic acid derivatives of this series were more potent than cisplatin in all the tumor cell lines tested. On the other hand, the IC_{50} values for oral keratinocyte cells (OKF6/TERT, nontumor cells) were

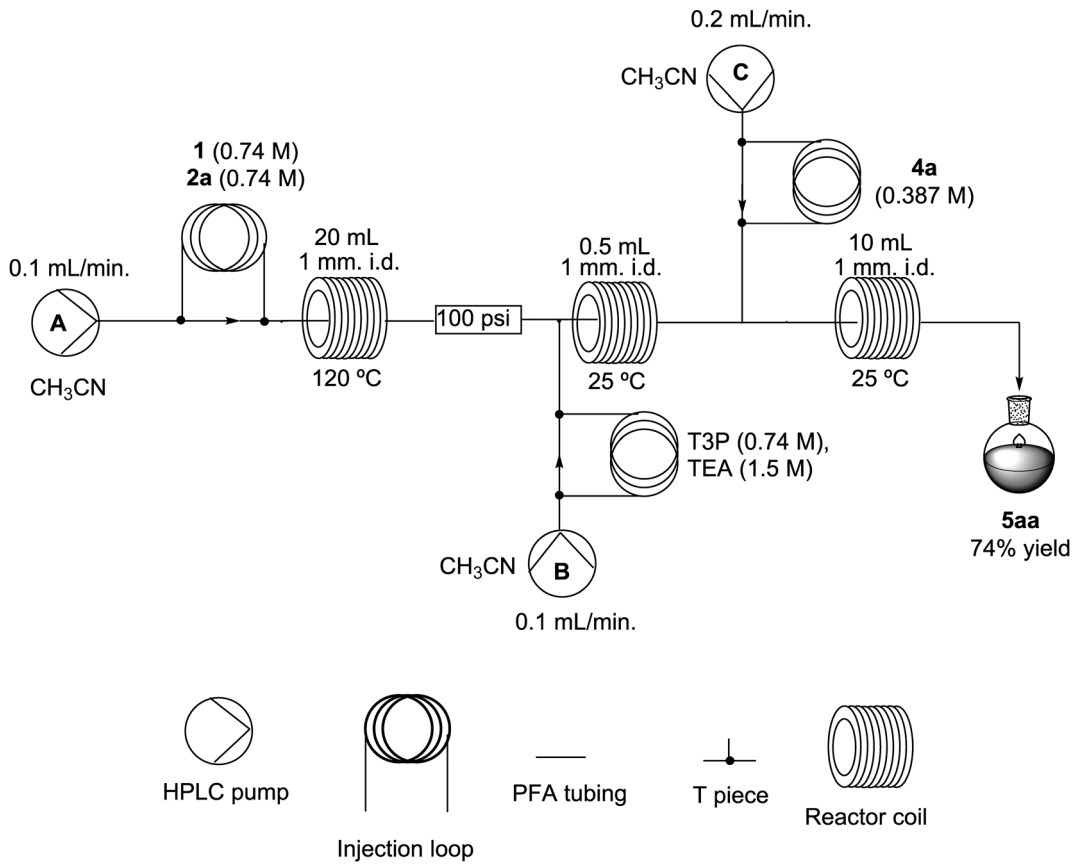

Fig. 4 Two-step flow sequence for the telescoped preparation of DLCs esters.

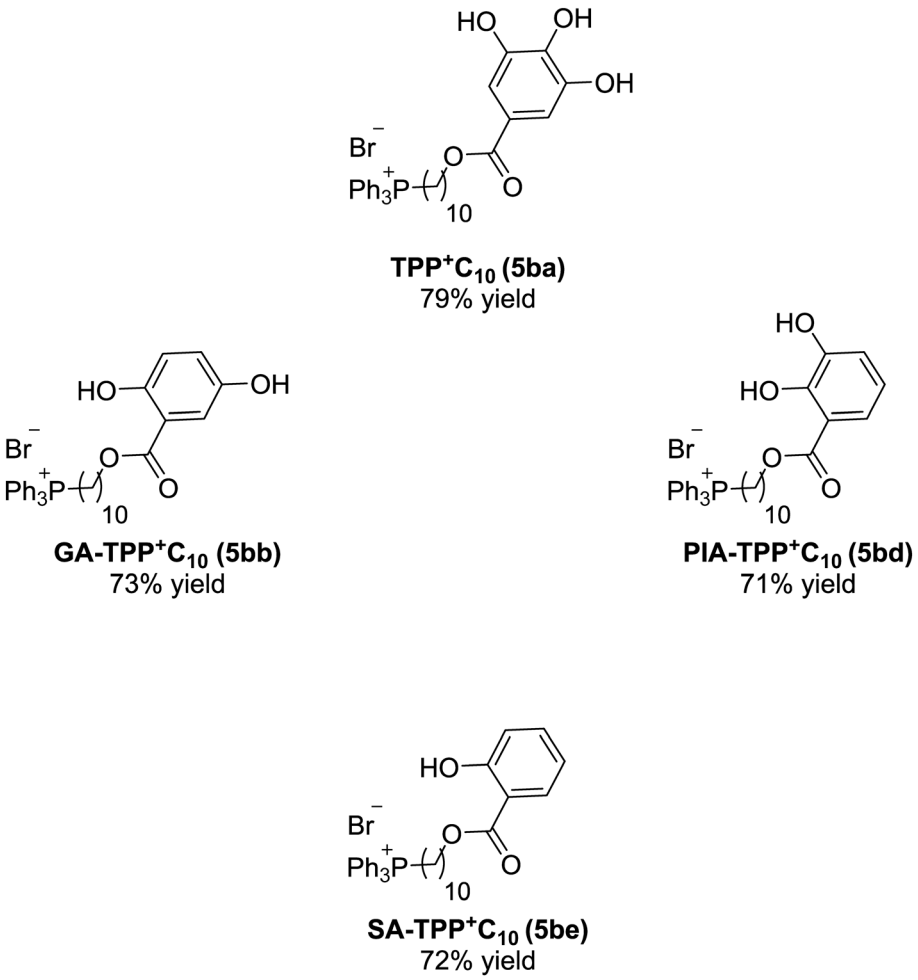

Fig. 5 Set of DLCs esters synthesized under flow regime.

significantly higher than those observed in the Cal-27 tumor cell line, thus showing that hydroxylated benzoic acid esters linked to TPP^+ are selective for the Cal-27 and SCC-15 cell lines (Table 4). In the case of **PIA-TPP$^+$C$_{10}$** (**5ba**) in HEp-2 cells, there is clearly no selectivity, as the IC_{50} values for laryngeal tumor cells are close to the IC_{50} values in the OKF-6/TERT non-tumor cells (Table 4).

Table 3 The cytotoxic effect of TPP^+-benzoates on HNSCC cell lines (Cal27, HEp-2, SCC-15) and oral keratinocyte (OKF-6/TERT), and selectivity index IC_{50} = the concentration required to induce cytotoxicity effects in 50% of HNSCC cells and oral keratinocyte cells after 48 h of treatment. Compounds **BA-C$_{10}$** (benzoic acid decyl ester), and **PIA-C$_{10}$** (2,3-dihydroxybenzoic acid decyl ester) were used as controls to evaluate the effects of inclusion of TPP^+ moiety in compounds (structures in Fig. 1). Each assay was performed in triplicate. Key: *$p \leq 0.05$ with respect to the effect of **TPP$^+$C$_{10}$** (3,4,5-trihydroxybenzoic acid decyl ester) at the same cell line time; ***$p \leq 0.001$ with respect to the effect of **TPP$^+$C$_{10}$** at the same cell line and time; $a = p \leq 0.05$ respect to the effect at the same time in Cal-27 cell line

	IC_{50} at 48 h (μM)			
	Cell lines			
Compounds	Cal-27	HEp-2	SCC-15	OKF-6/TERT
SA-TPP$^+$C$_{10}$ (**5be**)	2.3 ± 0.06*	4.28 ± 0.12	3.2 ± 0.2	12.7 ± 0.2^a
GA-TPP$^+$C$_{10}$ (**5bd**)	2.2 ± 0.02*	5.66 ± 1.09	2.7 ± 0.1*	13.2 ± 0.4^a
PIA-TPP$^+$C$_{10}$ (**5bb**)	1.6 ± 0.01*	8.28 ± 0.27	2.9 ± 0.07	7.5 ± 0.1^a
TPP$^+$C$_{10}$ (**5ba**)	3.4 ± 0.1	12.52 ± 0.94	3.0 ± 0.09	13.1 ± 0.4
Cisplatin (CDDP)	4.7 ± 0.9	5.2 ± 0.7	12.5 ± 1.2	3.2 ± 0.2

The results obtained in the SCC line suggest that every compound assayed exerted a cytotoxic effect with similar IC_{50} values (<2 μM after 72 h of incubation, Table S1 in the ESI†) and had similar selectivity. However, the IC_{50} values did not correlate with the number and position of the hydroxyl groups present on the benzoic acid moiety (pharmacophore group), although the values were significantly different compare to non-tumor cells ($p < 0.05$). According to results obtained previously for these compounds in breast cancer cells, it has been suggested that cytotoxic activity is achieved with the presence of at least one hydroxyl group as a substituent on benzoic acid.[3] Apparently, modification of the number of hydroxyl groups in the benzoic acid ring and their position does not significantly affect the cytotoxic activity in the tumor cells assessed. Furthermore, triphenylphosphine does not have cytotoxic activity in the cell lines assessed in this work (data not shown). Furthermore, the IC_{50} values of the hydroxylated benzoic acid derivatives were similar or

Table 4 Selectivity index for benzoates-TPP^+ derivatives at 48 h values were calculated from IC_{50} ratio between non-tumor cell and tumor cell lines from the respective sigmoidal dose–response curves

	Selectivity index (48 h)		
Compounds	OKF-6 TERT/Cal-27	OKF-6 TERT/HEp-2	OKF-6 TERT/SCC-15
SA-TPP^+C_{10} (5be)	5.5	3.0	4.0
GA-TPP^+C_{10} (5bd)	6.0	2.3	4.9
PIA-TPP^+C_{10} (5bb)	4.7	0.9	2.6
TPP^+C_{10} (5ba)	3.8	1.0	4.4
Cisplatin (CDDP)	<1.0	<1.0	<1.0

lower than the IC_{50} values for cisplatin, a gold standard therapy in HNSCC tumors (Table 3). Moreover, our compounds were more selective than cisplatin for tumor *versus* nontumor cells (Table 4).

2.2.2. Anticlonogenic effect of benzoic acid-derived lipophilic cations in Cal 27 cell line. In order to evaluate the consequences of inducing an antiproliferative effect in the Cal 27 cell line, we determined the effects of the benzoate derivatives on the clonogenic capacity of these cells. Fig. 6 shows that all the compounds tested were able to inhibit this capacity in a concentration-dependent manner (Fig. 6A–D).

2.2.3. Mechanism of action of benzoic acid-derived lipophilic cations in HNSCC cell lines. To determine the mechanism of action of the benzoic acid derivatives, we evaluated the mitochondrial oxygen consumption rate (OCR), $\Delta\Psi_m$ and intracellular levels of ATP after treatment of the cells with the different compounds (Fig. 7 and 8). The results from the OCR experiments (Fig. 7) suggest that all compounds were able to induce a mitochondrial uncoupling effect in a concentration-dependent manner in the tongue carcinoma cell line Cal-27 but with different efficacies (Fig. 7B–D). Indeed, **SA-TPP^+C_{10} (5be)** and **TPP^+C_{10} (5ba)** did not accomplish the maximal uncoupling effect induced by the classical uncoupling agent CCCP (Fig. 7B and E). However, **GA-TPP^+C_{10} (5bb)** and **PIA-TPP^+C_{10} (5bd)** did reach the maximal effect induced by CCCP (Fig. 7C and D). These uncoupling effects may be implicated in the selectivity of each compound, but more experiments are needed to establish the relationship.

The results show that the compounds exhibited OXPHOS uncoupling effects. However, the uncoupling effect of **SA-TPP^+C_{10} (5be)** and **TPP^+C_{10} (5ba)** was less potent than that of CCCP, the classical uncoupling agent. This could be favourable because it implies low toxicity of **SA-TPP^+C_{10} (5be)**

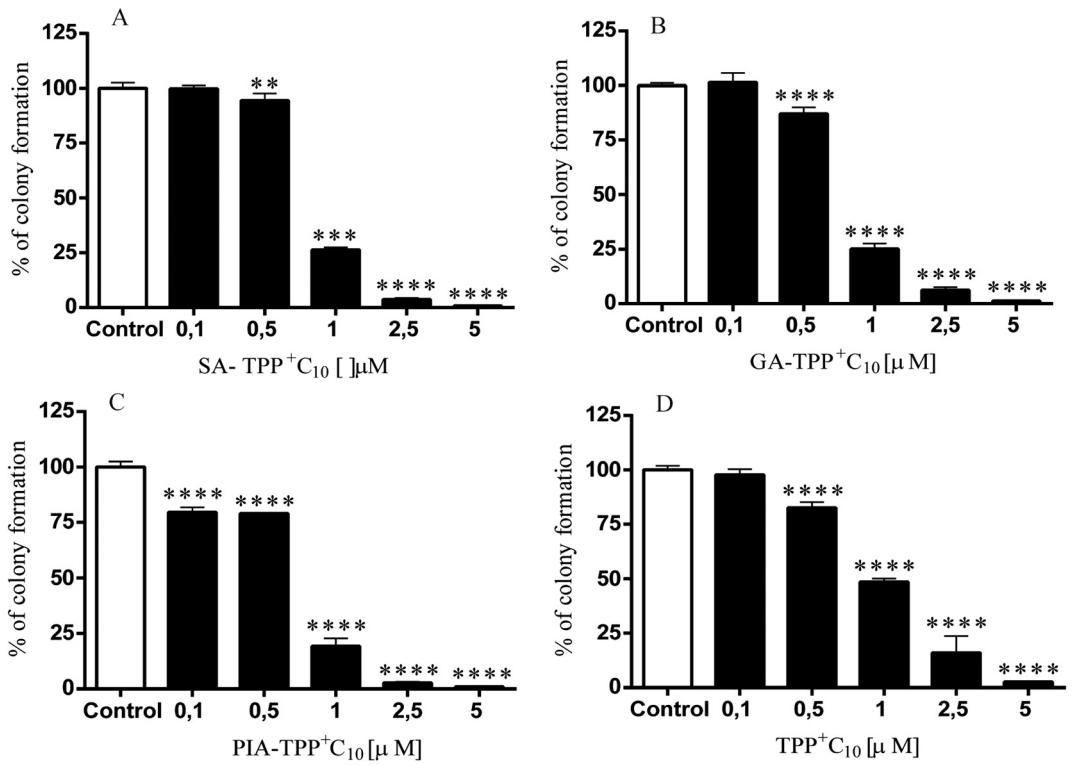

Fig. 6 Effects of benzoate-TPP^+ derivatives on the colony formation of HNSCC cells (Cal 27 cell line). Figures A–D shows quantification of 3 independent experiment of **SA-TPP^+C_{10} (5be)**, **GA-TPP^+C_{10} (5bb)**, **PIA-TPP^+C_{10} (5bd)**, and **TPP^+C_{10} (5ba)**, respectively. Data were compared to the control group through ANOVA followed by the Bonferroni post-test. Key: $*p < 0.05$, $**p < 0.01$ $***p < 0.001$.

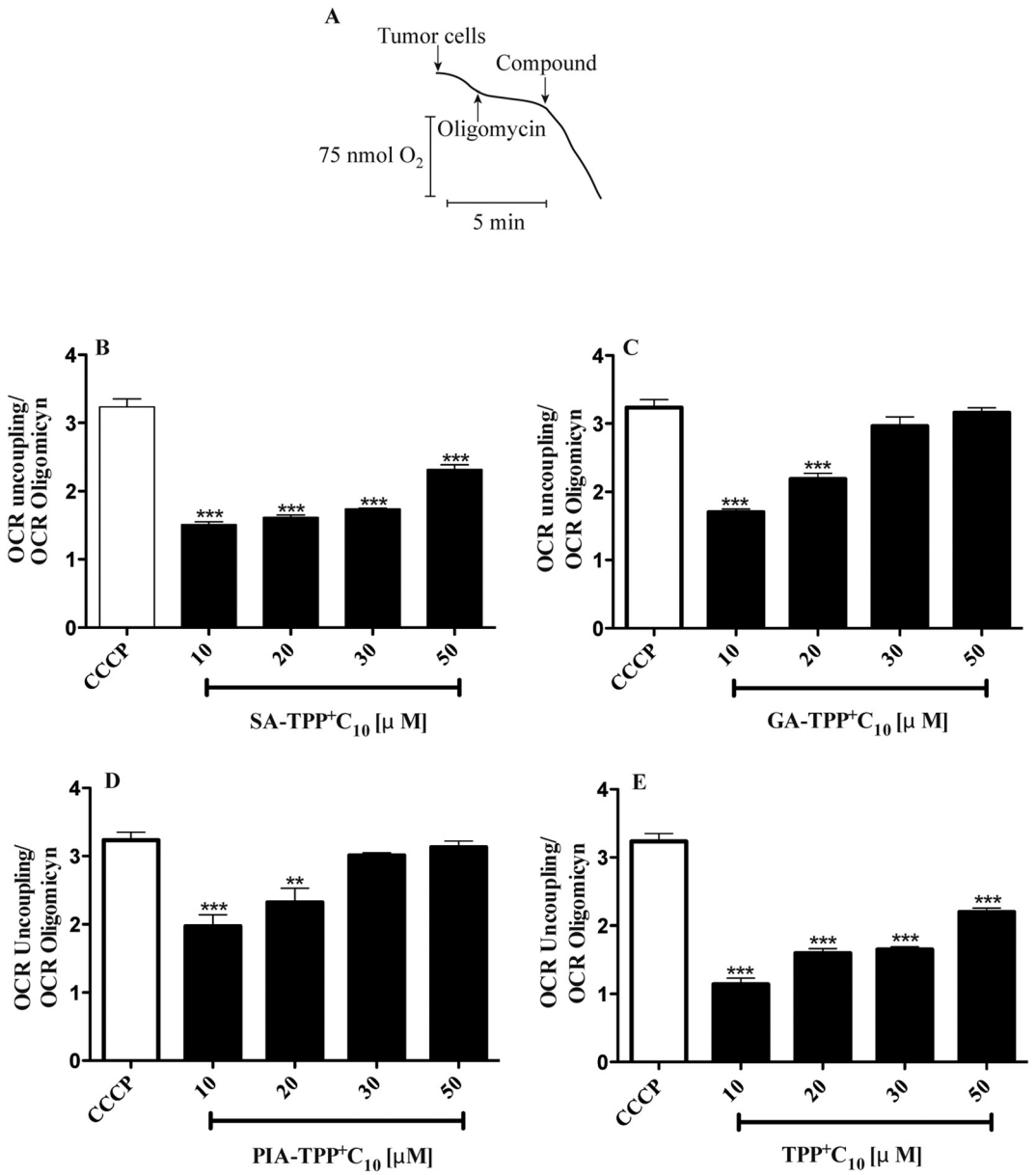

Fig. 7 Oxygen consumption rate. Tumour cell respiration was measured using a Clark electrode coupled to a personal computer. 5×10^6 Cal-27 cells were used per experimental measurement. 0.6 mL cell suspension in PBS (pH 7.4) at 25 °C, and then 8.3 mM of L-glutamine were added in the electrode chamber. Respiration rates were inhibited by 2.5 μg ml^{-1} oligomycin, and OXPHOS was fully uncoupled by 0.133 μM FCCP, used as a control of all experiments. Graph A shows a representative sequence of events for each experiment. Figures B–E show the uncoupling effects of **SA-TPP$^+$C$_{10}$** (**5be**), **GA-TPP$^+$C$_{10}$** (**5bb**), **PIA-TPP$^+$C$_{10}$** (**5bd**) and **TPP$^+$C$_{10}$** (**5ba**), respectively. The results shown are the averages of three independent assays ± SD. Data were compared to the control group (ANOVA) followed by the Bonferroni post-test. Key: *$p < 0.05$, **$p < 0.01$ ***$p < 0.001$.

and **TPP$^+$C$_{10}$** (**5ba**) in nontumor cells, as it is known that powerful uncoupling compounds such as FCCP, CCCP or 2,4-dinitrophenol produce nonselective necrotic or apoptotic death of normal cells, since all these compounds have been demonstrated low selectivity, with reduced effective concentration range.[29,30] However, recently it has been described new uncoupler agents with high potency and low selectivity, but this compound are chemically different to our benzoic acid lipophilic cations.[31] The mechanism of action proposed is different from that described for gallic acid derivatives because diverse authors have shown an apoptotic effect of GA derivatives through an increase in ROS production.[29] On the other hand, these results are comparable with the effects observed for the same molecules evaluated in parallel against colorectal cancer *in vitro*.[28]

Fig. 8 shows the decrease in both $\Delta\Psi_m$ and intracellular ATP levels caused by the action of the benzoic acid derivatives in the Cal-27 and HEp-2 cell lines. Fig. 8A and C show a decrease in $\Delta\Psi_m$ for all compounds assessed independent of the concentration used. All molecules induced similar potential decreases to 0.5 μM CCCP (maximal uncoupling effect). Nevertheless, the effects of the

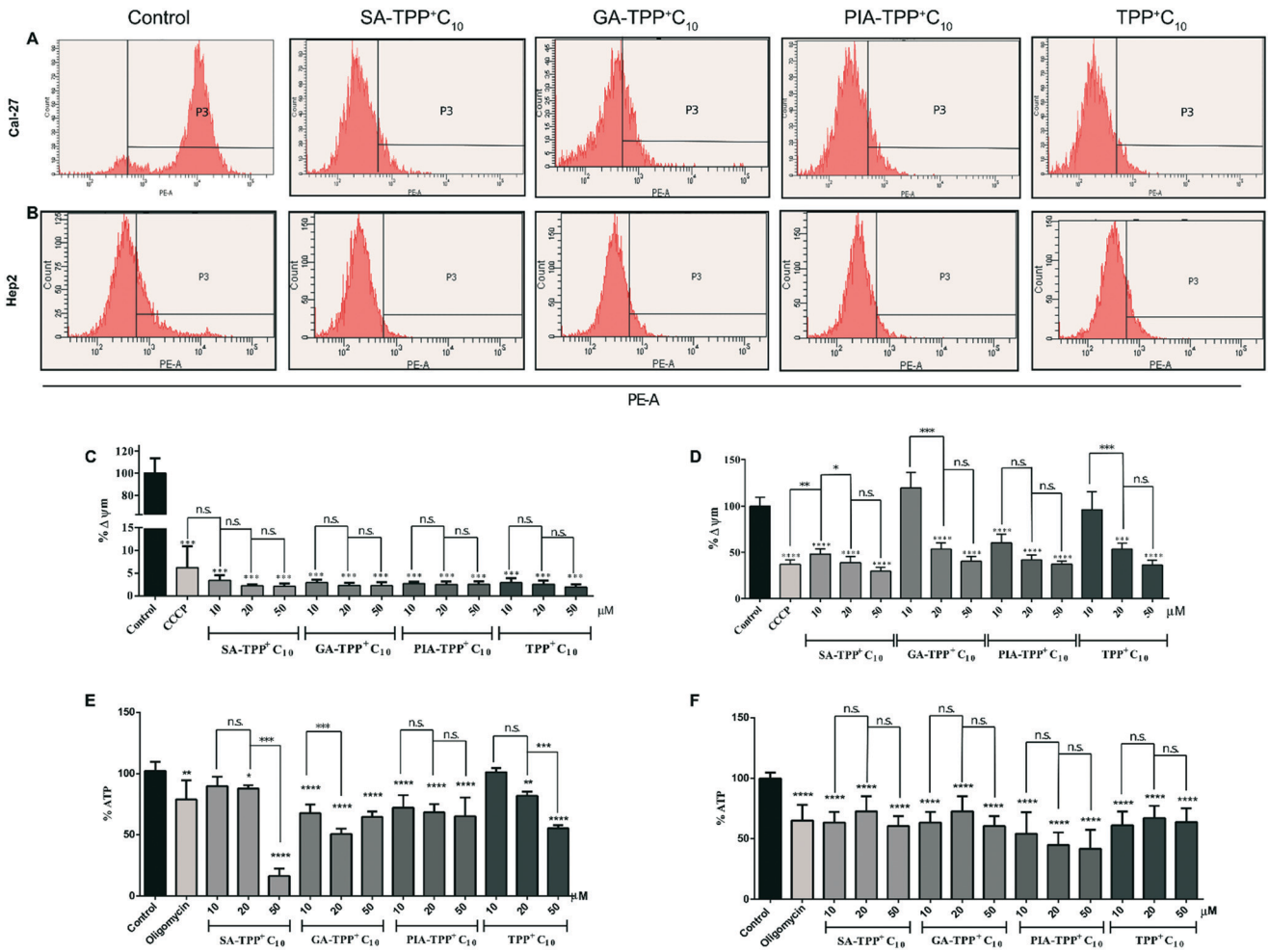

Fig. 8 Effects of hydroxybenzoate-TPP$^+$ derivatives on mitochondrial transmembrane potential and intracellular ATP levels. Panel A shows the representative histograms of the effects of hydroxybenzoate-TPP$^+$ derivatives on the mitochondrial transmembrane potential in CAL-27 cells. Panel B shows the corresponding effects in HEp-2 cells. Panels C and D represent the percent ratio of the concentration-dependent effects of all lipophilic cations with respect to controls in the Cal-27 and Hep-2 cell lines, respectively. Panels E and F similarly show the percent ratios of the effects for 4 h of incubation of each cation on ATP levels in Cal-27 and HEp-2 cells, respectively. The values shown are the mean values ± SD of at least three independent experiments. Data were compared to the control group through ANOVA followed by the Bonferroni post-test. Key: *$p < 0.05$, **$p < 0.01$ ***$p < 0.001$. N.S.: not statistical differences between groups.

lipophilic cations on the mitochondrial membrane potential of HEp-2 cells was less potent than that observed in Cal-27 cells (Fig. 8B and D). **SA-TPP$^+$C$_{10}$** (**5be**) and **PIA-TPP$^+$C$_{10}$** (**5bd**) showed a marked effect on mitochondrial potential, similar to that observed with CCCP. Moreover, the intracellular ATP contents decreased significantly in the Cal-27 cell line at each concentration tested for **GA-TPP$^+$C$_{10}$** (**5bb**) and **PIA-TPP$^+$C$_{10}$** (**5bd**) but not in a concentration-dependent manner (Fig. 8E).

Similarly, the ATP levels observed in HEp-2 cells were significantly reduced for all molecules, but the effects were not proportional to the molecule concentration under any of the conditions tested (Fig. 8F). Moreover, the data showed that uncoupling causes a decrease in ATP levels, but this decrease is lower than expected to induce cell death. This behaviour could be explained by the activation of compensatory mechanisms triggered in conditions of energy deprivation, such as the activation of adenylate kinase or AMPK (AMP-activated protein kinase).[32,33] Indeed, the uncoupling effects and the decrease in ATP levels and mitochondrial transmembrane potential, which are elicited by the TPP$^+$ derivatives, induce energy stress and selectively trigger tumor cell apoptosis. This cytotoxic mechanism may represent a new alternative for inducing cell death in tumor cells that are frequently multiresistant to chemotherapy and new biological drugs.[34–36]

2.2.4. Benzoic acid-derived lipophilic cations induce caspase 3 activation and apoptosis in HNSCC cell lines. Finally, we determined whether the hydroxybenzoate derivatives were able to induce apoptosis in the Cal-27 and HEp-2 cell lines. We used the IC_{50} and 2 × IC_{50} concentrations for this experiment, to guaranty the cell death effect, as we saw in the cytotoxicity assay. The results showed that all compounds were able to induce apoptosis at a similar level to the positive control staurosporine in the Cal-27 cell

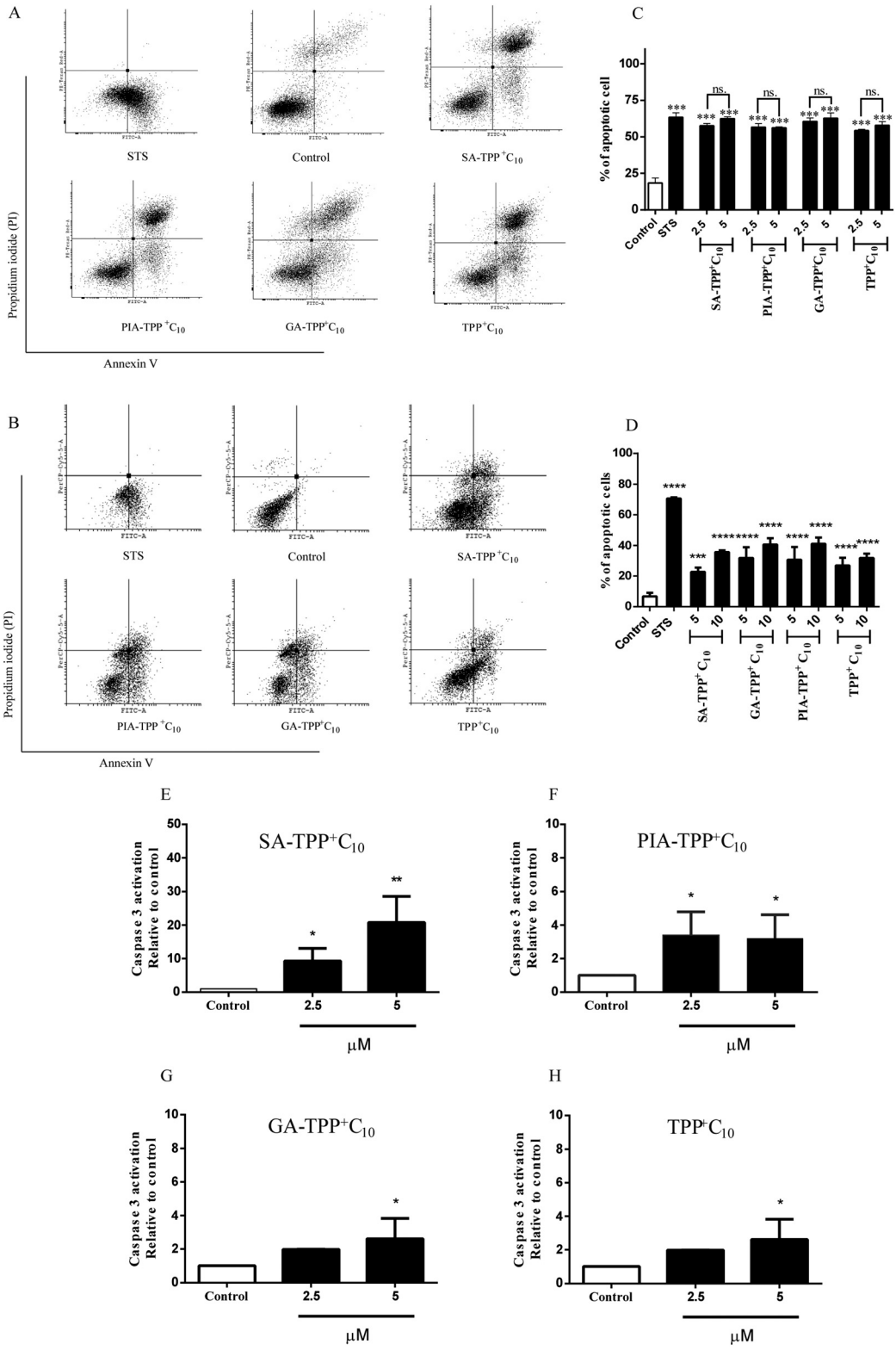

Fig. 9 Apoptosis and caspase 3 activation induced by hydroxybenzoate-TPP^+ compounds. Representative dot-plots of PI and annexin V double staining in Cal-27 cells (panel A) in the presence of 2.5 μM of each cation or 10 μM staurosporine (STS) as a positive control during 48 h of treatment. Panel C shows the quantification of apoptotic Cal-27 cells. Panel B shows representative dot-plots of PI and annexin V double staining in HEp-2 cells in the presence of 2.5 μM of each cation or 10 μM STS during 48 h of treatment. Panel D shows the quantification of apoptotic HEp-2 cells. The activation of caspase 3 was evaluated at 48 h of incubation at two concentrations of the compounds E) **SA-TPP^+C_{10}** (**5be**) F) **PIA-TPP^+C_{10}** (**5bd**) G) **GA-TPP^+C_{10}** (**5bb**) and H) **TPP^+C_{10}** (**5ba**), respectively. The values shown are the means ± SD of at least three independent experiments. The error bars show the 95% confidence interval. Data were compared to the control group through ANOVA followed by the Bonferroni post-test. Key: $*p < 0.05$, $**p < 0.01$ $***p < 0.001$; ns = no statistically significant difference.

line (Fig. 9A and C). The apoptosis death in Cal 27 seems not to be dependent of concentration, since at double concentrations did not increase the cell death twice (Fig. 9A and C). The percent of necrotic cells was not significant (approximately 5% after 48 h), except in the case of treatment with **PIA-TPP$^+$C$_{10}$** (**5bd**) and **GA-TPP$^+$C$_{10}$** (**5bb**) (approximately 10% for both compounds after 48 h, $p < 0.05$). Furthermore, the effects of hydroxybenzoic acid derivatives in HEp-2 cells were weaker than those induced by the classical apoptosis inducer staurosporine but significant with respect to the control (Fig. 9B and D). Similar to what was seen in Cal-27 cells, the apoptosis-inducing effects in HEp-2 cells was not concentration-dependent under our experimental conditions.

To evaluate whether the compounds triggered the classical apoptotic response, we also evaluated caspase 3 activation through flow cytometry. Fig. 9E–H show that each compound was able to induce caspase 3 activation in the Cal-27 cell line, which was not dependent on the concentration. These results suggest that hydroxybenzoate-TPP$^+$ derivatives induce apoptosis by activation of caspase 3 through the intrinsic pathway.

3. Conclusion

Regarding the relevance of reproducing the *in vitro* effects obtained and observing a significant antineoplastic effect in animal models for which more product with high purity is necessary, it is currently relevant to optimize synthetic routes for new organic compounds with biological activity, principally those that may reach effects at lower concentrations, which may be easily achieved in systemic circulation or in tissues. These kinds of molecules would be useful for the treatment of pathologies that actually present higher mortality and drug resistance rates, such as head and neck cancer. In this work, we optimized the continuous flow synthesis of up to five lipophilic cations, obtaining higher yields and better selectivity than the previous route while embracing the well-known advantages of performing reactions in a continuous fashion.

With respect to the biological results, it is known that head and neck cancers are highly lethal diseases, principally because they are diagnosed in their later stages, thus reducing the probability of successful treatments such as surgery, radiotherapy and chemotherapy. Currently, a few classical antitumor drugs are available as chemotherapy, which can be used in the advanced stages of the tumors. Indeed, in these patients, multimodal intervention is frequently required, involving the use of new chemotherapeutic drugs (such as monoclonal antibodies) that have a pivotal role. Unfortunately, the new strategies used in combination treatments for head and neck squamous cell carcinoma have experienced unexpected resistance. However, according to our results, energy stress induction, as a mechanism of action, may represent an alternative approach to induce death of tumor cells. Indeed, it is known that tumor cells are frequently multiresistant to both classical chemotherapeutic drugs and monoclonal antibodies. Furthermore, metabolic reprogramming appears to be a generalized phenomenon observed in many tumor cells and an important feature in multidrug resistant cells, which are present in solid tumors. In conclusion, our results offer a series of molecules that are able to exert potent cytotoxic effects in human tumor cell lines through the induction of energy stress. These compounds might be assessed *in vivo* either alone or in combination with old and new chemotherapeutic drugs in order to evaluate the possibility of improving current treatments.

Materials and methods

Chemicals and reagents

General procedures. Commercially available, laboratory grade reagents were used without further purification. High resolution mass spectrometry (HRMS, ESI$^+$) was measured with an Apex III FT ICR mass spectrometer (Bruker, Billerica, USA). ^{1}H-Nuclear magnetic resonance (NMR) spectra were recorded in $CDCl_3$, acetone-d_6, and DMSO-d_6 at room temperature with a Bruker AMX-400 spectrometer (Bruker, Billerica, USA) operating at 400.16 MHz with residual protic solvent as the internal reference (DMSO-d_6, δ = 2.50 ppm); chemical shifts (δ) are given in parts per million (ppm) and coupling constants (J) are given in Hertz (Hz). The proton spectra are reported as follows: δ (multiplicity, coupling constant J, number of protons). ^{13}C-NMR spectra were recorded in $CDCl_3$, and DMSO-d_6 at room temperature with the same spectrometer operating at 101.62 MHz with the central peak of DMSO-d_6 (δ = 39.50 ppm) as the internal reference. DEPT-135 pulse sequences were used to aid in the assignment of signals in the ^{13}C-NMR spectra. ^{31}P-NMR spectra were recorded in DMSO-d_6 at room temperature with the same spectrometer operating at 162.13 MHz with triphenylphosphine (δ = −7.00 ppm) as the internal reference. Analytical TLC was performed on Merck silica gel 60 F_{254} chromatofoils. The purification of all products was carried out on silica gel and the solvents used are specified in each case.

DMEM culture medium, carbonylcyanide *m*-chlorophenylhydrazone (CCCP), glutamine, glucose, 3-(4,5-dimethylthiazol-2-yl)-2,5-diphenyltetrazolium bromide (MTT), dimethyl sulfoxide (DMSO), fetal bovine serum (FBS), staurosporine, and trypan blue 0.4% solution, were purchased from Sigma Chemical Co. (St. Louis, MO). Cisplatin was purchased from Santa Cruz Biotechnology. Penicillin/streptomycin and trypsin, were purchased from Hyclone Laboratories (South Logan, UT). All other reagents were purchased from Sigma (Sigma-Aldrich, USA).

*Triphenyl(11-ol-undecyl)phosphonium bromide (**3a**)*

General procedure for the continuous-flow synthesis of phosphonium salts. A solution containing triphenylphosphine (0.74 M in CH_3CN) and 11-bromo-1-undecanol (0.74 M in CH_3CN) was reacted at 120 °C in a 20

mL PFA reactor coil (0.1 mL min^{-1}). The outcome stream was collected during 5 min (steady state regime) and solvent was evaporated under reduced pressure to isolate 187 mg (98%) of colourless oil identified as triphenyl(11-ol-undecyl) phosphonium bromide (***n***). **^{1}H NMR** (400 MHz, $CDCl_3$): δ 7.94–7.69 (m, 15H), 3.67 (t, J = 6.6 Hz, 2H), 1.65–1.57 (m, 6H), 1.30–1.24 (m, 14H) ppm. **^{31}P NMR** (162 MHz, DMSO-d_6): δ 24.04 ppm. **MS** (ESI) m/z (%) 435.27, 434.27, 433.27 (100, M^+–Br).

*Triphenyl(10-ol-decyl)phosphonium bromide (**3b**).* Following the general procedure previously described for the continuous-flow synthesis of phosphonium salts the reaction of triphenylphosphine (0.74 M in CH_3CN) and 10-bromo-1-decanol (0.74 M in CH_3CN) afforded, after collection during 5 min (steady state regime) 181 mg (99%) of a colourless oil identified as triphenyl(10-ol-decyl)phosphonium bromide (***n***). **^{1}H NMR** (400 MHz, $CDCl_3$): δ 7.91–7.59 (m, 15H), 3.62 (t, J = 6.7 Hz, 2H), 1.70–1.11 (m, 18H) ppm. **^{31}P NMR** (162 MHz, DMSO-d_6): δ 24.03 ppm. **MS** (ESI) m/z (%) 421.26, 420.26, 419.25 (100, M^+–Br).

*Triphenyl(11-((3,4,5-trihydroxybenzoyl)oxy)-undecyl) phosphonium bromide (**TPP$^+$C$_{11}$, 5aa**)*

General procedure for the stepwise continuous-flow synthesis of lipophilic phosphonium bromide-benzoic acid derivatives. A solution containing triphenylphosphine (0.74 M in CH_3CN) and 11-bromo-1-undecanol (0.74 M in CH_3CN) was reacted at 120 °C in a 20 mL PFA reactor coil (0.1 mL min^{-1}). The outcome stream was collected during 5 min (steady state regime) and solvent was evaporated under reduced pressure to isolate 176 mg (92%) of colourless oil identified as triphenyl(11-ol-undecyl)phosphonium bromide (***n***). The crude was then redissolved in CH_3CN (3.2 mL, 0.1 M in CH_3CN) and T3P® (0.20 mL, 50% w/w in DMF) and triethylamine (0.09 mL) were added. The resulting mixture was flowed (0.2 mL min^{-1}) to react with a solution of gallic acid (**4a**) (57 mg) in CH_3CN (3.4 mL, 0.1 M in CH_3CN) in a 10 mL coiled reactor at room temperature. The outstream solution was collected, solvent was removed under reduced pressure and the obtained oily residue purified by chromatographic column (silica gel, DCM/MeOH 5%) to isolate 192 mg of a light yellow oil (85% isolated yield) identified as triphenyl(11-((3,4,5-trihydroxybenzoyl)oxy)-undecyl)phosphonium bromide (**TPP$^+$C$_{11}$, 5aa**).

^{1}H NMR (400 MHz, DMSO-d_6): δ 7.95–7.76 (m, 15H, ArH), 7.10 (s, 2H, ArH), 4.22 (t, J = 6.3 Hz, 2H), 1.74–1.29 (m, 20H) ppm. **^{31}P NMR** (162 MHz, DMSO-d_6): δ 24.04 ppm. **MS** (ESI) m/z (%) 587.27, 586.27, 585.27 (100, M^+–Br).

General procedure for the telescoped synthesis of lipophilic phosphonium bromide-benzoic acid derivatives. A solution containing triphenylphosphine (0.74 M in CH_3CN) and 11-bromo-1-undecanol (0.74 M in CH_3CN) was reacted at 120 °C in a 20 mL PFA reactor coil (0.1 mL min^{-1}). The outcoming stream was combined in a T-piece (each stream running at 0.1 mL min^{-1}) with a solution containing a previously mixed combination of T3P (0.74 M in CH_3CN) and Et_3N (1.5 M in CH_3CN) and allowed to mix at rt in a 0.5 mL PFA reactor coil. The combined stream was then combined in a T-piece with a solution gallic acid (0.387 M in CH_3CN) (0.2 mL min^{-1}) and reacted at rt in a 10 mL PFA reactor coil. The outstream solution was collected during 5 min (steady state regime) and the residue purified by column chromatography (silica gel, DCM/MeOH 5%) to isolate 182 mg of a light yellow oil (74% isolated yield) identified as triphenyl(11-((3,4,5-trihydroxybenzoyl)oxy)-undecyl)phosphonium bromide (**TPP$^+$C$_{11}$, 5aa**).

*Triphenyl(10-((3,4,5-trihydroxybenzoyl)oxy)-decyl) phosphonium bromide (**TPP$^+$C$_{10}$, 5ba**).* Following the general procedure for the preparation of lipophilic phosphonium bromide derivatives, the reaction of triphenylphosphine, 10-bromo-1-decanol, T3P, Et_3N, and gallic acid, afforded after collecting during 5 min (steady state regime) 190 mg (79%) of a colorless oil identified as triphenyl(10-((3,4,5-trihydroxybenzoyl)ozy)-decyl)phosphonium bromide (**TPP$^+$C$_{10}$, 5ba**).

^{1}H NMR (400 MHz, DMSO-d_6): δ 7.90–7.73 (m, 15H, ArH), 6.98 (s, 2H, ArH), 4.12 (t, J = 6.2 Hz, 2H), 1.62–1.17 (m, 18H) ppm. **^{13}C NMR** (100 MHz, DMSO-d_6): δ 170.87 (s), 166.36 (s), 146.00 (s), 138.80 (s), 135.30 (d, J_{C-P} = 3.0 Hz), 134.05 (d, J_{C-P} = 10.0 Hz), 130.68 (d, J_{C-P} = 12.0 Hz), 120.04 (s), 119.05 (s, J_{C-P} = 85.0 Hz), 109.04 (d), 64.30 (t), 30.13 (t, J_{C-P} = 17.0 Hz), 29.19 (t), 29.04 (t), 28.99 (t), 28.71 (t), 28.55 (t), 25.92 (t), 22.22 (t, J_{C-P} = 4.0 Hz), 20.72 (t, J_{C-P} = 5.0 Hz) ppm. **^{31}P NMR** (162 MHz, DMSO-d_6): δ 24.03 ppm. **HRMS** calcd for $C_{35}H_{40}O_5P$: 571.2608, found: 571.2610.

*Triphenyl(10-((2,5-dihydroxybenzoyl)oxy)-decyl)phosphonium bromide (**GA- TPP$^+$C$_{10}$, 5bb**).* Following the general procedure for the preparation of lipophilic phosphonium bromide derivatives, the reaction of triphenylphosphine, 10-bromo-1-decanol, T3P, Et_3N, and gentisic acid, afforded after collecting during 5 min (steady state regime) 150 mg (73%) of a colourless oil identified as triphenyl(10-((2,5-dihydroxybenzoyl)oxy)-decyl)phosphonium bromide (**GA-TPP$^+$C$_{10}$, 5bb**).

^{1}H NMR (400 MHz, DMSO-d_6): δ 9.99 (s, 1H), 9.25 (s, 1H), 7.83–7.76 (m, 15H, ArH), 7.18 (d, J = 1.8 Hz, 1H, ArH), 7.00 (dd, J = 8.7 and 1.8 Hz, 1H, ArH), 6.80 (d, J = 8.6 Hz, 1H), 4.27 (t, J = 6.2 Hz, 2H), 1.70–1.21 (m, 18H). **^{13}C NMR** (100 MHz, DMSO-d_6): δ 169.45 (s), 153.75 (s), 150.08 (s), 135.31 (d, J_{C-P} = 3.0 Hz), 134.06 (d, J_{C-P} = 10.0 Hz), 130.68 (d, J_{C-P} = 13.0 Hz), 124.37 (d), 119.06 (s, J_{C-P} = 85.1 Hz), 118.53 (d), 114.55 (d), 112.92 (s), 65.52 (t), 30.19 (t, J_{C-P} = 16.0 Hz), 29.19 (t), 29.06 (t), 28.99 (t), 28.53 (t), 28.42 (t), 25.83 (t), 22.20 (t, J_{C-P} = 4.0 Hz), 20.69 (t, J_{C-P} = 5.0 Hz) ppm. **^{31}P NMR** (162 MHz, DMSO-d_6): δ 24.07 ppm. **HRMS** calcd for $C_{35}H_{40}O_4P$: 555.2659, found: 555.2668.

*Triphenyl(10-((2,3-dihydroxybenzoyl)oxy)-decyl)phosphonium bromide (**PIA-TPP$^+$C$_{10}$, 5bd**).* Following the general procedure for the preparation of lipophilic phosphonium bromide derivatives, the reaction of triphenylphosphine, 10-bromo-1-decanol, T3P, Et_3N, and 2,3-dihydroxybenzoic acid, afforded after collecting during 5 min (steady state regime) 146 mg (71%) of a colourless oil identified as triphenyl(10-((2,3-

dihydroxybenzoyl)oxy)-decyl)phosphonium bromide (**PIA-TPP$^+$C$_{10}$, 5bd**).

^{1}H NMR (400 MHz, DMSO-d_6): δ 7.12–6.90 (m, 15H), 6.51 (dd, J = 8.1 and 1.6 Hz, 1H), 6.20 (dd, J = 7.9 and 1.6 Hz, 1H), 5.93 (t, J = 8.0 Hz, 1H), 4.26 (t, J = 6.5 Hz, 2H), 1.06–0.30 (m, 18H) ppm. **^{13}C NMR** (100 MHz, DMSO-d_6): δ 162.30 (s), 141.77 (s), 137.59 (s), 126.74 (d, J_{C-P} = 3.0 Hz), 125.3 (d, J_{C-P} = 9.9 Hz), 122.03 (d, J_{C-P} = 12.5 Hz), 111.93 (s, J_{C-P} = 50.6 Hz), 110.93 (d), 110.58 (d), 110.08 (d), 104.56 (s), 57.10 (t), 22.02 (t, J_{C-P} = 16.0 Hz), 20.81 (t), 20.66 (t, J_{C-P} = 4.3 Hz), 20.30 (t), 20.05 (t), 17.47 (t), 14.02 (t, J_{C-P} = 4.6 Hz), 13.48 (t), 12.97 (t) ppm. **^{31}P NMR** (162 MHz, DMSO-d_6): δ 24.04 ppm. **HRMS** calcd for $C_{35}H_{40}O_4P$: 555.2659, found: 555.2668.

*Triphenyl(10-((2-hydroxybenzoyl)oxy)-decyl)phosphonium bromide (**SA- TPP$^+$C$_{10}$, 5be**).* Following the general procedure for the preparation of lipophilic phosphonium bromide derivatives, the reaction of triphenylphosphine, 10-bromo-1-decanol, T3P, Et_3N, and salicylic acid, afforded after collecting during 5 min (steady state regime) 165 mg (72%) of a colourless oil identified as triphenyl(10-((2-hydroxybenzoyl)oxy)-decyl)phosphonium bromide (**SA-TPP$^+$C$_{10}$, 5be**).

^{1}H NMR (400 MHz, DMSO-d_6): δ 10.56 (s, 1H), 7.91–7.73 (m, 16H, ArH), 7.51–7.47 (m, 1H), 6.98–6.93 (m, 1H), 6.91–6.89 (m, 1H), 4.27 (t, J = 6.3 Hz, 2H), 1,68–1,14 (m, 18H) ppm. **^{13}C NMR** (100 MHz, DMSO-d_6): δ 169.39 (s), 160.63 (s), 135.30 (d, J_{C-P} = 2.0 Hz), 134.07 (d, J_{C-P} = 10.0 Hz), 130.68 (d, J_{C-P} = 13.0 Hz), 130.28 (d), 119.84 (d), 119.07 (s, J_{C-P} = 86.1 Hz), 117.82 (d), 113.46 (s), 65.61 (t), 30.17 (t, J_{C-P} = 17.0 Hz), 29.19 (t), 29.07 (t), 28.99 (t), 28.58 (t), 28.40 (t), 25.82 (t), 22.26 (t, J_{C-P} = 4.0 Hz), 20.76 (t, J_{C-P} = 5.0 Hz) ppm. **^{31}P NMR** (162 MHz, DMSO-d_6): δ 24.03 ppm. **HRMS** calcd for $C_{35}H_{40}O_3P$: 539.2710, found: 539.2706.

Cell lines and cell culture

The human oral squamous cell lines, Cal-27 (ATCC® CRL2095™) and SCC15 (ATCC® CRL1623™) were acquired from the American type culture collection (ATCC). The laryngeal cell line HEp-2 was acquired from the Instituto de Salud Pública de Chile. Normal human oral keratinocyte cells OKF-6/Tert-2, were kindly donated by Dr. Denise Bravo (Faculty of Dentistry, Universidad de Chile). Cal-27 and HEp-2 cell lines were grown in DMEM supplemented with 10% FBS, 100 U mL^{-1} of penicillin and 100 μg mL^{-1} of streptomycin in a humidified 5% CO_2 atmosphere at 37 °C. SCC-15 cells were grown in a 1 : 1 mixture of Dulbecco's modified Eagle's medium and Ham's F12 medium containing 1.2 g L^{-1} sodium bicarbonate, 2.5 mM L-glutamine, 15 mM HEPES and 0.5 mM sodium pyruvate supplemented with 400 ng mL^{-1} hydrocortisone and fetal bovine serum 10%. Oral keratinocytes were grown in keratinocyte serum-free medium (KSFM) (Gibco®) supplemented with bovine pituitary extract, hEGF (0.2 ng mL^{-1}), $CaCl_2$ (0.3 mM) and 100 U mL^{-1} penicillin, and 100 μg mL^{-1} streptomycin in a humidified 5% CO_2 atmosphere at 37 °C. For passages, cells were detached by using trypsin-EDTA and seeded in culture plates for different experiments.

Cell viability assay

Cells were seeded into a 96-well plate (1 × 10^4 cell per well). After 24 h, benzoate-TPP$^+$ compounds were added at increasing concentrations into the wells and incubated for 24, 48 and 72 h. After this time, the cells were washed twice with PBS (phosphate buffered saline) 1×, and then 100 μL of 0.5 mg mL^{-1} MTT solution was added to each well. After 2 h of incubation, MTT was removed and the formazan crystals were dissolved in 40 μL of DMSO. Absorbance was measured at 570 nm with a microplate ELISA reader (Infinite F50® Tecan Group Ltd., Swiss).

Oxygen consumption assay

The cell respiration rates were measured polarographically.[2] Tumour cells were cultured at 80% of confluence and then trypsinized and counted. 5 × 10^6 cells were used for experimental measurement. 0.6 mL of cell suspension in PBS (pH 7.4) at 25 °C was added to the electrode chamber with L-glutamine (8.3 mM). The respiration rate which accounts for the OXPHOS system was firstly inhibited by 2.5 μg mL^{-1} oligomycin. Then, the full uncoupled respiration rates were assessed adding 0.133 μM of CCCP (carbonyl cyanide *m*-chlorophenylhydrazine), which was used as control. The increase of oxygen consumption rates (OCR) caused by each compound under study were measured by adding increasing concentrations of each. The results were compared with the OCR for CCCP.

Mitochondrial transmembrane potential ($\Delta\Psi_m$)

Changes in transmembrane potential ($\Delta\Psi_m$) were determined using tetramethylrhodamine methyl ester (TMRM) as a probe. Cells were seeded into 24-well plates (1 × 10^5 cells per well) for 24 h and then incubated with 200 nM TMRM. Cells were immediately exposed to increasing concentrations of each compound (2.5 to 30 μM) for 30 min. After washing with PBS, cells were detached and suspended in cold PBS for analysis by flow cytometry FACS (FACSAria® III, BD Biosciences) at a wavelength of 540Ex/595Em nm.

Intracellular ATP levels

The tumour cell ATP levels were measured using the CellTitle-Glo Luminescent Assay (Promega, Madison, WI) according to the manufacturer's instructions. Briefly, 1 × 10^4 cells per well were seeded into a 96-well plate, and were cultured during 24 h. Each well was stimulated with the compounds at different concentrations for 4 h. Then, 100 μL of the cell suspension were transferred to an opaque 96-well plate and incubated at room temperature for 10 min in the dark. Finally, the luminescence was captured using a Thermo-Scientific Varioskan Flash spectral scanning reader. As a control assay for cell viability and cell membrane

integrity for the measurement of intracellular ATP content, PI incorporation was assessed by flow cytometry (FACS Canto, BD Biosciences, San Jose, CA)[37] according to previously described.[1]

Colony assay

For this assay 1×10^3 cells were cultured in a 6-well plate. Then, the cells were incubated during 24 h at 37 °C under 5% CO_2. Later the cells were treated for 24 h with different concentrations of each compound. Then, the culture medium was replaced with culture medium without compound, and the cells were incubated for further 120 h. Finally, crystal violet (0.5% in methanol) was applied to the cells for 30 min. The number of colonies was photographed and determined by using ImageJ software program (NIH, Bethesda, MD, USA).[38]

Apoptosis

The induction of apoptosis by the benzoic acid derivatives was determined through flow cytometry using annexin V and PI probes (annexin V-FITC apoptosis detection kit, Abcam), according to the manufacturer's instructions (FACS Canto, BD Biosciences). Briefly, 1×10^5 cells per mL were incubated with the lipophilic cations for 48 h at 37 °C under 5% CO_2. The cells were suspended in 500 μL of 1× annexin V-binding buffer, 5 μL of both annexin V and PI were added to the samples which then were incubated for 5 min at room temperature. The samples were measured at Ex/Em = 488/530 nm for annexin V-FITC and Ex/Em = 488/575 nm for PI (Miao *et al.*, 2014)[39] and 10 000 events were recorded. The results were analyzed using the Cyflogic program (non-commercial version, CyFlo Ltd.).

Caspase 3 activation

Activation of caspase 3 was determined using a PE Active Caspase-3 apoptosis kit (BD, Franklin Lakes, NJ) according to the manufacturer's protocol. Briefly, 5×10^5 cells per well were seeded in 24-well plates for 24 h, at 37 °C. Cells were then incubated with various concentrations of the compounds for 24 h. Cells were detached and suspended in cell permeability/fixation buffer and incubated for 30 min in the dark at 4 °C. Cells were centrifuged and washed once with cell-staining buffer, then centrifuged and suspended in anti-caspase PE antibody and incubated for 30 min in the dark. Finally, cells were washed once with cell-staining buffer and analyzed by flow cytometry at 488Ex/617Em nm and the data were analyzed using Cyflogic software (non-commercial version, CyFlo Ltd.).

Statistical analysis

The results were analysed by one or two-way ANOVA with an *ad hoc* post-test. The IC_{50} values were calculated using a dose–response curve with a variable slope. The differences were considered significant at $p < 0.05$.

Funding

This work was supported by U-INICIA grant from the Vicerrectoría de Investigación y Desarrollo, Universidad de Chile. [Grant U-INICIA-2014-82379] (JAJ), Fondecyt Iniciación Grant No. 11180533 (JAJ), Fondecyt Iniciación grant No. 11160281 (MC), Fondecyt Iniciación Grant No. 11170962 and Fondecyt Regular grant No. 1180296 (JF and JAJ).

Role of the funding source

The funders did not interfere in any of the stages of the preparation of this manuscript.

Statement of contributions

VCC, JG and MD planned and performed, and JAS planned and coordinated the organic chemical synthesis of the compounds. MC, JA, IO, CP, MV, AM and JAJ performed biological evaluation. JF, AM and RRF support the experiment realized. MC and JAJ planned and coordinated the biological assays. All authors contributed to manuscript revision, read and approved the submitted version.

Conflicts of interest

The authors declare that the research was conducted in the absence of any commercial or financial relationships that could be construed as a potential conflict of interest.

Acknowledgements

MD and JAS acknowledge Prof. Robert Stockman for the generous loan of a R2–R4 Vapourtec Flow Reactor, and Prof. Rosana Álvarez and Prof. Ángel R. de Lera for their continuous support.

Notes and references

1 J. A. Jara, V. Castro-Castillo, J. Saavedra-Olavarría, L. Peredo, M. Pavanni, F. Jaña, M. E. Letelier, E. Parra, M. I. Becker, A. Morello, U. Kemmerling, J. D. Maya and J. Ferreira, Antiproliferative and uncoupling effects of delocalized, lipophilic, cationic gallic acid derivatives on cancer cell lines. Validation in vivo in singenic mice, *J. Med. Chem.*, 2014, **57**, 2440–2454, DOI: 10.1021/jm500174v.

2 C. Frey, M. Pavani, G. Cordano, S. Muñoz, E. Rivera, J. Medina, A. Morello, J. Diego and J. Ferreira, Comparative cytotoxicity of alkyl gallates on mouse tumor cell lines and isolated rat hepatocytes ☆, *Comp. Biochem. Physiol., Part A: Mol. Integr. Physiol.*, 2007, **146**, 520–527, DOI: 10.1016/j.cbpa.2006.03.007.

3 C. Sandoval-acuna, S. Fuentes-retamal, D. Guzmán-rivera, L. Peredo-silva, M. Madrid-rojas, S. Rebolledo, V. Castro-castillo, M. Pavani, M. Catalán, J. Diego, J. A. Jara, E. Parra, G. M. Calaf, H. Speisky and J. Ferreira, Destabilization of mitochondrial functions as a target against breast cancer progression : Role of TPP + −linked-polyhydroxybenzoates, *Toxicol. Appl. Pharmacol.*, 2016, **309**, 2–14, DOI: 10.1016/j.taap.2016.08.018.

4 T. Tanaka and R. Ishigamori, Understanding carcinogenesis for fighting oral cancer, *J. Oncol.*, 2011, **2011**, 603740, DOI: 10.1155/2011/603740.
5 I. S. Fernández, P. Cuevas, J. Angulo, P. López-Navajas, Á. Canales-Mayordomo, R. González-Corrochano, R. M. Lozano, S. Valverde, J. Jiménez-Barbero, A. Romero and G. Giménez-Gallego, Gentisic acid, a compound associated with plant defense and a metabolite of aspirin, heads a new class of in vivo fibroblast growth factor inhibitors, *J. Biol. Chem.*, 2010, **285**, 11714–11729, DOI: 10.1074/jbc.M109.064618.
6 S. Tsao, T. Hsia and M. Yin, Protocatechuic Acid Inhibits Lung Cancer Cells by Modulating FAK, MAPK, and NF- κ B Pathways, *Nutr. Cancer*, 2014, **66**, 1331–1341, DOI: 10.1080/01635581.2014.956259.
7 P. J. Benny, G. Shibumon, K. Sunny and G. Cincy, 2,3-Dihydroxybenzoic Acid : An Effective Antifungal Agent Isolated from Flacourtia inermis Fruit, *Int. J. Pharm. Clin. Res.*, 2010, **2**, 101–105.
8 B. Alcalde, M. Granados and J. Saurina, Exploring the antioxidant features of polyphenols by spectroscopic and electrochemical methods, *Antioxidants*, 2019, **8**(11), 523, DOI: 10.3390/antiox8110523.
9 R. Gérardy, N. Emmanuel, T. Toupy, V. E. Kassin, N. N. Tshibalonza, M. Schmitz and J. C. M. Monbaliu, Continuous Flow Organic Chemistry: Successes and Pitfalls at the Interface with Current Societal Challenges, *Eur. J. Org. Chem.*, 2018, **2018**, 2301–2351, DOI: 10.1002/ejoc.201800149.
10 M. Baumann and I. R. Baxendale, Batch and Flow Synthesis of Pyrrolo[1,2-a]-quinolines via an Allene-Based Reaction Cascade, *J. Org. Chem.*, 2015, **80**, 10806–10816, DOI: 10.1021/acs.joc.5b01982.
11 B. Gutmann, P. Elsner, A. O'Kearney-Mcmullan, W. Goundry, D. M. Roberge and C. O. Kappe, Development of a Continuous Flow Sulfoxide Imidation Protocol Using Azide Sources under Superacidic Conditions, *Org. Process Res. Dev.*, 2015, **19**, 1062–1067, DOI: 10.1021/acs.oprd.5b00217.
12 M. Baumann, T. S. Moody, M. Smyth and S. Wharry, A Perspective on Continuous Flow Chemistry in the Pharmaceutical Industry, *Org. Process Res. Dev.*, 2020, DOI: 10.1021/acs.oprd.9b00524.
13 M. B. Plutschack, B. Pieber, K. Gilmore and P. H. Seeberger, The Hitchhiker's Guide to Flow Chemistry â¥, *Chem. Rev.*, 2017, **117**, 11796–11893, DOI: 10.1021/acs.chemrev.7b00183.
14 S. Kobayashi, Flow "fine" Synthesis: High Yielding and Selective Organic Synthesis by Flow Methods, *Chem.: Asian J.*, 2016, **11**, 425–436, DOI: 10.1002/asia.201500916.
15 S. V. Ley, D. E. Fitzpatrick, R. M. Myers, C. Battilocchio and R. J. Ingham, Machine-Assisted Organic Synthesis, *Angew. Chem., Int. Ed.*, 2015, **54**, 10122–10136, DOI: 10.1002/anie.201501618.
16 D. T. McQuade and P. H. Seeberger, Applying flow chemistry: Methods, materials, and multistep synthesis, *J. Org. Chem.*, 2013, **78**, 6384–6389, DOI: 10.1021/jo400583m.
17 D. Webb and T. F. Jamison, Continuous flow multi-step organic synthesis, *Chem. Sci.*, 2010, **1**, 675–680, DOI: 10.1039/c0sc00381f.
18 R. Porta, A. Puglisi, G. Colombo, S. Rossi and M. Benaglia, Continuous-flow synthesis of primary amines: Metal-free reduction of aliphatic and aromatic nitro derivatives with trichlorosilane, *Beilstein J. Org. Chem.*, 2016, **12**, 2614–2619, DOI: 10.3762/bjoc.12.257.
19 H. G. Jolliffe and D. I. Gerogiorgis, Chemical Engineering Research and Design Process modelling and simulation for continuous pharmaceutical manufacturing of ibuprofen, *Chem. Eng. Res. Des.*, 2014, **97**, 175–191, DOI: 10.1016/j.cherd.2014.12.005.
20 S. D. Schaber, D. I. Gerogiorgis, R. Ramachandran, J. M. B. Evans, P. I. Barton and B. L. Trout, Economic analysis of integrated continuous and batch pharmaceutical manufacturing: A case study, *Ind. Eng. Chem. Res.*, 2011, **50**, 10083–10092, DOI: 10.1021/ie2006752.
21 D. Medicine, C. N. Waer, P. Kaur, Z. Tumur, D. D. Hui, B. Le, C. Guerra, B. Henson, D. Seleem and J. Lewis, Rosmarinic Acid / Blue Light Combination Treatment Inhibits Head and Neck Squamous Cell Carcinoma In Vitro, *Anticancer Res.*, 2020, **758**, 751–758, DOI: 10.21873/anticanres.14006.
22 N. Beech, S. Robinson, S. Porceddu and M. Batstone, Dental management of patients irradiated for head and neck cancer, *Aust. Dent. J.*, 2014, **59**, 20–28, DOI: 10.1111/adj.12134.
23 D. L. Browne, B. J. Deadman, R. Ashe, I. R. Baxendale and S. V. Ley, Continuous Flow Processing of Slurries: Evaluation of an Agitated Cell Reactor, *Org. Process Res. Dev.*, 2011, **15**, 693–697, DOI: 10.1021/op2000223.
24 C. Battilocchio, I. R. Baxendale, M. Biava, M. O. Kitching and S. V. Ley, A Flow-Based Synthesis of 2-Aminoadamantane-2-carboxylic Acid, *Org. Process Res. Dev.*, 2012, **16**, 798–810, DOI: 10.1021/op300084z.
25 P. Filipponi, A. Gioiello and I. R. Baxendale, Controlled Flow Precipitation as a Valuable Tool for Synthesis, *Org. Process Res. Dev.*, 2016, **20**, 371–375, DOI: 10.1021/acs.oprd.5b00331.
26 R. L. Hartman, Managing Solids in Microreactors for the Upstream Continuous Processing of Fine Chemicals, *Org. Process Res. Dev.*, 2012, **16**, 870–887, DOI: 10.1021/op200348t.
27 M. F. Sainz, J. A. Souto, D. Regentova, M. K. G. Johansson, S. T. Timhagen, D. J. Irvine, P. Buijsen, C. E. Koning, R. A. Stockman and S. M. Howdle, A facile and green route to terpene derived acrylate and methacrylate monomers and simple free radical polymerisation to yield new renewable polymers and coatings, *Polym. Chem.*, 2016, **7**, 2882–2887, DOI: 10.1039/c6py00357e.
28 J. A. Jara, D. Rojas, V. Castro-Castillo, S. Fuentes-Retamal, C. Sandoval-Acuña, E. Parra, M. Pavani, J. D. Maya, J. Ferreira and M. Catalán, Novel benzoate-lipophilic cations selectively induce cell death in human colorectal cancer cell lines, *Toxicol. In Vitro*, 2020, **65**, 104814, DOI: 10.1016/j.tiv.2020.104814.
29 J. Grundlingh, P. I. Dargan, M. El-Zanfaly and D. M. Wood, 2,4-Dinitrophenol (DNP): A Weight Loss Agent with Significant Acute Toxicity and Risk of Death, *J. Med. Toxicol.*, 2011, **7**, 205–212, DOI: 10.1007/s13181-011-0162-6.

30 A. Kamour, N. George, D. Gwynnette, G. Cooper, D. Lupton, M. Eddleston, J. P. Thompson, J. A. Vale, H. K. R. Thanacoody, S. Hill and S. H. L. Thomas, Increasing frequency of severe clinical toxicity after use of 2,4-dinitrophenol in the UK: A report from the National Poisons Information Service, *Emerg. Med. J.*, 2015, **32**, 383–386, DOI: 10.1136/emermed-2013-203335.

31 E. S. Childress, J. M. Salamoun, S. R. Hargett, S. J. Alexopoulos, S.-Y. Chen, D. P. Shah, J. Santiago-Rivera, C. J. Garcia, Y. Dai, S. P. Tucker, K. L. Hoehn and W. L. Santos, [1,2,5]Oxadiazolo[3,4-b]pyrazine-5,6-diamine Derivatives as Mitochondrial Uncouplers for the Potential Treatment of Nonalcoholic Steatohepatitis, *J. Med. Chem.*, 2020, **63**(5), 2511–2526.

32 P. Dzeja and A. Terzic, Adenylate kinase and AMP signaling networks: metabolic monitoring, signal communication and body energy sensing, *Int. J. Mol. Sci.*, 2009, **10**, 1729–1772, DOI: 10.3390/ijms10041729.

33 Y. Wu, M. Sarkissyan, E. Mcghee, S. Lee and J. V. Vadgama, Combined inhibition of glycolysis and AMPK induces synergistic breast cancer cell killing, *Breast Cancer Res. Treat.*, 2015, **151**, 529–539, DOI: 10.1007/s10549-015-3386-3.

34 T. M. Brand, M. Iida, A. P. Stein, K. L. Corrigan, C. M. Braverman, N. Luthar, M. Toulany, P. S. Gill, R. Salgia, R. J. Kimple and D. L. Wheeler, AXL mediates resistance to cetuximab therapy, *Cancer Res.*, 2014, **74**, 5152–5164, DOI: 10.1158/0008-5472.CAN-14-0294.

35 C.-C. Hung, C.-Y. Chien, W.-F. Chiang, C.-S. Lin, T.-C. Hour, H.-R. Chen, L.-F. Wang, J.-Y. Ko, C.-H. Chang and J. Y.-F. Chen, P22Phox Confers Resistance To Cisplatin, By Blocking Its Entry Into the Nucleus, *Oncotarget*, 2015, **6**, 4110–4125, DOI: 10.18632/oncotarget.2893.

36 X. Li, Y. Lu, H. Lu, J. Luo, Y. Hong and Z. Fan, AMPK-mediated energy homeostasis and associated metabolic effects on cancer cell response and resistance to cetuximab, *Oncotarget*, 2015, **6**, 11507–11518.

37 M. M. Moisenovich, V. A. Ol'Shevskaya, T. I. Rokitskaya, A. A. Ramonova, R. G. Nikitina, A. N. Savchenko, V. V. Tatarskiy, M. A. Kaplan, V. N. Kalinin, E. A. Kotova, O. V. Uvarov, I. I. Agapov, Y. N. Antonenko and A. A. Shtil, Novel photosensitizers trigger rapid death of malignant human cells and rodent tumor transplants via lipid photodamage and membrane permeabilization, *PLoS One*, 2010, **5**, 1–13, DOI: 10.1371/journal.pone.0012717.

38 G. Fu, R. T. Somasundaram, F. Jessa and G. Srivastava, ER maleate is a novel anticancer agent in oral cancer: Implications for cancer therapy, *Oncotarget*, 2016, **7**(13), 17162–17181.

39 L. Miao, C. Liu, J. Ge, W. Yang, J. Liu, W. Sun, B. Yang, C. Zheng, H. Sun and Q. Hu, Antitumor Effect of TRAIL on Oral Squamous Cell Carcinoma using Magnetic Nanoparticle-Mediated Gene Expression, *Cell Biochem. Biophys.*, 2014, **69**, 663–672, DOI: 10.1007/s12013-014-9849-z.

